Near-Horizon Scrambling Membranes: A Minimal Phenomenological Waveform Model for Dissipative Horizonless Compact Objects

John Reimer Morales[1, *]

[1] *Independent Researcher*

(Dated: March 30, 2026)

I. INTRODUCTION

The direct detection of gravitational waves from coalescing compact binaries [1] has opened a precision window on the strong-field dynamics of black holes. Among the most fundamental questions accessible to gravitational-wave astronomy is whether the compact objects observed in these mergers possess event horizons—one-way causal boundaries from which no signal can escape—or whether the horizon is replaced by some form of physical surface or boundary layer.

This question is not merely philosophical. A classical event horizon is an idealization of general relativity (GR) that becomes singular in the interior and encounters deep tensions with quantum mechanics through the information paradox [2]. A substantial body of theoretical work has explored alternatives in which the horizon is replaced by a physical structure: gravastars with de Sitter interiors and thin-shell boundaries [3, 4], fuzzballs in string theory [5], firewalls and complementarity proposals [6, 7], and various phenomenological exotic compact object (ECO) models with partially reflective near-horizon surfaces [8–10].

Gravitational-wave observations provide three main channels for discriminating between black holes and horizonless alternatives: (i) conservative tidal response during inspiral, where the vanishing of static Love numbers for Kerr black holes in four-dimensional vacuum GR [11, 12] contrasts with the generically nonzero response of material or exotic compact objects; (ii) dissipative tidal heating, where infalling energy is absorbed by the horizon or by a near-horizon membrane, with distinct heating signatures for different boundary conditions [13–15]; and (iii) ringdown structure, where horizonless objects can produce modified quasinormal mode spectra and late-time echoes through near-horizon cavities [8, 17, 18].

Current observational results are consistent with GR black holes. The LIGO-Virgo-KAGRA (LVK) catalog places tight constraints on tidal deformability [19], increasingly constrains tidal heating [20], and has produced null results in echo searches [21–23]. At the same time, strongly reflective near-horizon surfaces face theoretical challenges: spinning ultracompact objects with high reflectivity are vulnerable to ergoregion instabilities [24, 25], and population-level analyses further constrain the reflective regime [27].

These results collectively point toward a specific corner of the ECO parameter space that remains viable: objects that are *almost* black holes—nearly perfectly absorptive, with membrane-like surfaces extremely close to the would-be horizon, producing small deviations observable only in precision data. This is the corner that the NHSM model is designed to occupy.

The key physical distinction is between a *point of no return* (classical event horizon) and a *point of no entry* (dissipative membrane): infalling matter and radiation are absorbed, scrambled, and effectively stored in membrane degrees of freedom rather than crossing into a classical interior. The membrane paradigm of Thorne, Price, and Macdonald [28] already treats the horizon as an effective dissipative surface for external observers; the NHSM model posits that this membrane is a physical surface, parameterizes its microstructure, and derives the waveform consequences.

This paper is organized as follows. Section II presents the physical picture and the four-parameter characterization of the NHSM object. Section III develops the explicit waveform ansatz, including the three constitutive laws and tapering rules. Section IV specifies recommended priors and consistency constraints. Section V demonstrates the model's behavior through synthetic injections and provides a Fisher-matrix detectability forecast. Section VI discusses compatibility with existing observational bounds. Section VII places the model in the broader ECO literature, and Sec. VIII summarizes.

Throughout, we clearly distinguish between established results drawn from the gravitational-wave and compact-object literature and the toy-model constitutive laws that are original to this work.

a. Notation and conventions. We use geometric units $G = c = 1$ for the theoretical development (Secs. II–III), with masses expressed in solar masses $M_\odot$ and the conversion factor $M_\odot \simeq 4.926 \times 10^{-6}\,\mathrm{s}$ applied where frequencies are quoted in Hz. Distances are in Mpc. The power spectral density of detector noise is quoted in the standard convention [Hz^{-1}].

* jrm@globalharmonics.org

II. THE NHSM MODEL

A. Physical picture

We consider a compact object with three layers:

1. **Exterior**: a Kerr (or Schwarzschild, for nonspinning systems) vacuum spacetime for $r > r_{\rm m}$. Strictly, a membrane with nonzero surface stress-energy sources a non-Kerr correction to the exterior metric through the junction conditions; for $\epsilon \ll 1$ this correction is subdominant and we neglect it at leading order.

2. **Membrane**: a timelike worldtube at
$$r_{\rm m} = r_+(1+\epsilon), \quad 0 < \epsilon \ll 1, \tag{1}$$
where r_+ is the would-be horizon radius of a Kerr black hole with the same mass and spin.

3. **Interior**: a regular core. The simplest toy choice is a de Sitter-like equation of state $p_{\rm in} = -\rho_{\rm in}$, but the waveform model developed in this paper depends only on the membrane's effective parameters, not on the specific interior solution.

This construction is closely related to the gravastar family of models [3, 4] but differs in one critical respect: the membrane is *strongly dissipative* rather than reflective. This choice is motivated by three considerations. First, highly reflective near-horizon surfaces are increasingly constrained by LVK data and population-level analyses [27]. Second, spinning ultracompact objects with high reflectivity face ergoregion instabilities [24, 25]: quenching the instability at spin $\chi \lesssim 0.9$ requires absorptivity exceeding approximately 6%, while stability at arbitrary spin requires $\gtrsim$ 60% absorption [24]. Third, the fast-scrambling conjecture [30, 31] suggests that if the membrane carries microscopic degrees of freedom, it should process incoming information rapidly—absorbing and scrambling rather than coherently reflecting.

The membrane's surface stress-energy tensor is governed by the Israel junction conditions [29]:
$$[K_{ab}] - \gamma_{ab}[K] = -8\pi S_{ab}, \tag{2}$$
where γ_{ab} is the induced metric on the membrane, K_{ab} is the extrinsic curvature, and brackets denote the jump across the shell. For a physically useful membrane, S_{ab} includes surface energy density σ, surface pressure p_s, shear and bulk viscosities η and ζ, and a microstructure term $\tau_{ab}^{\rm micro}$ providing an effective phenomenological encoding of information processing and scrambling.

Rather than working with the full stress-energy content of the membrane (which would require a specific microscopic model), we adopt a phenomenological approach: we characterize the membrane's macroscopic response through four effective parameters that connect directly to gravitational-wave observables. The physical picture is illustrated in Fig. 1.

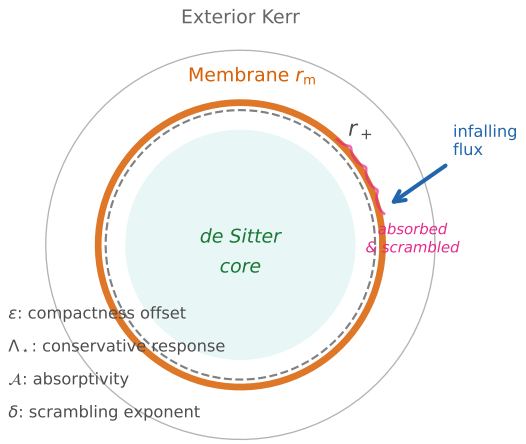

FIG. 1. Physical picture of the NHSM object. Exterior Kerr spacetime (outer circle) is matched to a dissipative membrane (solid orange, at $r_{\rm m} = r_+(1+\epsilon)$) just outside the would-be horizon r_+ (dashed). Infalling flux is absorbed and scrambled by the membrane rather than crossing into the interior. A de Sitter-like core (shaded) is the simplest toy choice for the regular interior; the waveform model is independent of this choice. The four NHSM parameters and their physical roles are listed.

B. The four parameters

We parameterize the NHSM object by
$$\Theta_{\rm NHSM} = \{\epsilon,\ \Lambda_\star,\ \mathcal{A},\ \delta\}. \tag{3}$$

Their physical meanings are:

a. Compactness offset ϵ. This controls how close the membrane sits to the would-be horizon, via Eq. (1). Smaller ϵ corresponds to higher compactness and more BH-like behavior. The parameter enters the waveform primarily through the near-horizon cavity timescale
$$\tau_{\rm c} = \kappa_\tau\, M_{\rm f}\, |\ln \epsilon|, \tag{4}$$
where $M_{\rm f}$ is the final (remnant) mass and κ_τ is an $O(1)$ constant set to $\kappa_\tau = 4$ in the minimal model. The logarithmic dependence on ϵ arises from the standard near-horizon tortoise-coordinate cavity picture: for an object with a surface at $r_{\rm m} = r_+(1+\epsilon)$, the proper cavity depth in the tortoise coordinate scales as $\Delta r_* \propto M|\ln\epsilon|$.

b. Conservative response amplitude $\Lambda_\star$. This is an effective tidal-response parameter controlling the conservative (non-dissipative) inspiral dephasing. In vacuum four-dimensional GR, Schwarzschild and Kerr black holes have exactly vanishing static tidal Love numbers [11, 12]. Compact material objects and ECOs generically have nonzero Love numbers, though for ultracompact objects approaching the Schwarzschild radius the deviation is logarithmically suppressed [35,

36]. The parameter $\Lambda_\star$ can take either sign, since non-BH compact objects need not have the same sign conventions as ordinary neutron-star tidal response [16].

c. Absorptivity $\mathcal{A}$. This is a normalized membrane absorption efficiency with $\mathcal{A} = 1$ corresponding to BH-like perfect absorption and $\mathcal{A} = 0$ to the fully reflective limit. In the inspiral sector, $\mathcal{A}$ controls dissipative heating—the energy deposited in the membrane by the tidal interaction, which is the direct analog of tidal heating at the horizon in GR [13–15]. In the ringdown sector, $\mathcal{A}$ determines the membrane reflectivity and hence the strength of any late-time cavity structure. For spinning systems, $\mathcal{A}$ is bounded from below by ergoregion stability requirements [24].

d. Scrambling exponent δ. This is a frequency-dependent response exponent controlling how the membrane processes information at different scales. It enters both the conservative response (through a microtexture filter that suppresses high-frequency tidal coupling) and the reflectivity (through frequency-dependent scrambling suppression). Physically, $\delta = 1$ corresponds to simple Debye-like exponential relaxation, $0 < \delta < 1$ to stretched-exponential long-memory behavior characteristic of glassy or hierarchically organized systems, and $\delta > 1$ to sharper UV suppression. The microtexture filter $\Xi_\delta(f) = [1 + (2\pi f\,\tau_{\rm c})^\delta]^{-1}$ is structurally a Mittag-Leffler-type relaxation function, which arises naturally from anomalous diffusion on substrates with nontrivial spectral dimension [39]. We emphasize that δ is a *spectral/microstate* parameter, not a claim that macroscopic spacetime has a noninteger dimension. Using a single δ across both the conservative and reflectivity sectors is a minimality assumption: one microstructure exponent governs both responses. This is the model's strongest simplifying hypothesis, and data may eventually require independent exponents (see Sec. VII).

C. Entropy and information architecture

The entropy structure of the membrane is not derived from a specific microscopic model; rather, it provides phenomenological motivation for the scrambling exponent δ. For the leading entropy, we retain the Bekenstein-Hawking area law [33, 34]:

$$S_{\rm mem}(L) = \frac{A}{4\ell_{\rm P}^2}\left[1 + \alpha\left(\frac{\ell_*}{L}\right)^\delta + \cdots\right], \tag{5}$$

where A is the membrane area, ℓ_* is the membrane microstructure scale, L is the coarse-graining scale, and α is a dimensionless coefficient. The subleading correction encodes the frequency-dependent microstructure parameterized by δ; this is one possible motivation for the appearance of a fractional exponent in the constitutive laws. However, the precise relationship between the microstructure of any entropy correction and the frequency-dependent response encoded in the waveform constitutive laws (Sec. III) remains to be established. The present model treats δ as a single effective parameter capturing this connection at leading order. No waveform observable in this paper depends directly on Eq. (5).

TABLE I. The four NHSM parameters, their physical roles, prior ranges, and primary observational channels.

Param.	Role	Prior	Channel
ϵ	Compactness	10^{-20}–10^{-3}	All (via $\tau_{\rm c}$)
$\Lambda_\star$	Conservative	$\lvert\Lambda_\star\rvert \lesssim 20$	Inspiral
$\mathcal{A}$	Absorptivity	[0, 1]	Heat. + ring.
δ	Scrambling	[0.25, 1.75]	Microtexture

Scrambling proceeds on a timescale $t_{\rm scr} \sim \beta \ln S$ [30–32], consistent with the membrane operating near the fast-scrambling bound. The cavity time $\tau_{\rm c}$ defined in Eq. (4) sets the time for a signal to traverse the near-horizon cavity; the scrambling time determines how rapidly the membrane redistributes the deposited information across its degrees of freedom.

III. WAVEFORM ANSATZ

A. Overview and validity envelope

The NHSM waveform is defined as a small deformation of a standard calibrated BBH frequency-domain waveform template. The model is constructed for quasi-circular, nonprecessing (or mildly spinning) binaries in the regime where deviations from the BBH baseline are perturbatively small. The validity envelope is

$$\epsilon \ll 1, \quad |\Lambda_\star| \lesssim O(1), \quad \mathcal{A} \gtrsim \mathcal{A}^{\rm min}(\chi_{\rm f}), \quad \delta > 0. \tag{6}$$

Let $\tilde{h}_{\rm base}(f;\boldsymbol{\vartheta})$ denote any calibrated BBH frequency-domain waveform model (e.g., IMRPhenomD for nonspinning systems, IMRPhenomXAS for aligned spin), with standard source parameters $\boldsymbol{\vartheta} = \{m_1, m_2, \chi_1, \chi_2, D_L, \iota, \phi_c, t_c, \ldots\}$.

The membrane-deformed waveform is

$$\boxed{\tilde{h}_{\rm NHSM}(f) = \tilde{h}_{\rm base}(f;\boldsymbol{\vartheta})\,\exp\!\left[i\,\Delta\Psi(f)\right] \times \left[1 + W_R(f)\,\mathcal{T}(f)\right]} \tag{7}$$

where $\Delta\Psi(f)$ is a phase deformation active during inspiral and late inspiral, and $\mathcal{T}(f)$ is a transfer-function correction active in the ringdown. The factorization into a phase deformation and a multiplicative ringdown correction follows the structure of existing ECO waveform frameworks: conservative and dissipative tidal effects are best constrained in the inspiral sector [13–15], while postmerger ECO effects are naturally represented through near-horizon transfer functions [8, 17, 18].

B. Inspiral phase deformation

The total phase deformation is

$$\Delta\Psi(f) = W_\Lambda(f)\,\Delta\Psi_\Lambda(f) + W_\mathcal{A}(f)\,\Delta\Psi_\mathcal{A}(f), \quad (8)$$

where W_Λ and $W_\mathcal{A}$ are smooth tapering windows (defined in Sec. III D).

1. Conservative tidal correction

The conservative sector uses the standard tidal phase basis from compact-binary waveform models:

$$\Delta\Psi_\Lambda(f) = \Lambda_{\rm eff}(f)\,\Phi^{\rm lib}_{\rm tidal}(f;\boldsymbol{\vartheta}), \quad (9)$$

where $\Phi^{\rm lib}_{\rm tidal}$ is the leading-order tidal phase basis familiar from neutron-star binary modeling (scaling as v^{10} at leading PN order, with $v = (\pi M f)^{1/3}$), and $\Lambda_{\rm eff}(f)$ is an effective tidal deformability that encodes the NHSM membrane response.

We propose the following constitutive law:

$$\boxed{\Lambda_{\rm eff}(f) = \frac{\Lambda_\star}{|\ln\epsilon|}\,\frac{1}{1+(2\pi f\,\tau_{\rm c})^\delta}.} \quad (10)$$

This is a *toy-model closure relation*, not an established result. Its structure encodes three physical features:

1. The prefactor $1/|\ln\epsilon|$ reflects the logarithmic compactness suppression of Love numbers for ultracompact objects as the surface approaches the horizon [35, 36]. For $\epsilon = 10^{-8}$ this gives a suppression factor of $\sim 1/18$.

2. The amplitude $\Lambda_\star$ sets the overall scale of conservative response, with $\Lambda_\star = 0$ recovering the BH limit of vanishing tidal deformability.

3. The frequency-dependent factor $\Xi_\delta(f) = [1 + (2\pi f\,\tau_{\rm c})^\delta]^{-1}$ is a microtexture filter: at low frequencies ($f \ll 1/\tau_{\rm c}$) the membrane responds quasistatically, while at high frequencies the scrambling dynamics suppress the coherent tidal response. This is consistent with the general principle, supported by membrane-paradigm analyses of compact-object tidal response [16], that the effective tidal coupling is frequency-dependent.

2. Dissipative heating correction

For the dissipative sector, we reuse the existing BH-heating phase basis rather than inventing a new flux law:

$$\Delta\Psi_\mathcal{A}(f) = \mathcal{A}\,\Phi^{\rm lib}_{\rm heat}(f;\boldsymbol{\vartheta}), \quad (11)$$

where $\Phi^{\rm lib}_{\rm heat}$ is taken from a heating-capable BBH waveform model.

This is the channel that encodes the "no entry" character of the membrane: the inspiral flux is absorbed and thermalized with efficiency $\mathcal{A}$, rather than being reflected (as in a hard-wall ECO) or lost through the horizon (as in a classical BH). The parameter $\mathcal{A} = 1$ recovers the BH-like heating level.[1]

For nonspinning systems up to merger, the 2025 merger-capable frequency-domain heating approximant [15] provides a validated heating basis. For aligned-spin exploratory analyses, the generic tidal-heating phase basis motivated by worldline EFT [13, 14] can be used at lower frequencies with appropriate tapering.

C. Ringdown transfer function

For the postmerger sector, we use a weak-cavity transfer function:

$$\mathcal{T}(f) = \frac{R(f)\,e^{i(2\pi f\,\tau_{\rm c}+\phi_0)}}{1 - R(f)\,e^{i(2\pi f\,\tau_{\rm c}+\phi_0)}}, \quad (12)$$

with $\phi_0 = 0$ in the minimal four-parameter model. This structure follows the standard ECO logic [8, 17]: an ultracompact horizonless object produces BH-like prompt ringdown, with later deviations governed by radiation bouncing between the photon-sphere potential barrier and the near-horizon surface, with each round trip accumulating a phase $2\pi f\,\tau_{\rm c}$ and losing amplitude through the frequency-dependent reflectivity $R(f)$.

The reflectivity constitutive law is:

$$\boxed{R(f) = \sqrt{1-\mathcal{A}}\,\exp\!\big[-(2\pi f\,\tau_{\rm c})^\delta\big].} \quad (13)$$

This is a *toy-model closure*, chosen for four properties:

1. When $\mathcal{A} \to 1$, $R \to 0$: BH-like perfect absorption, with no appreciable echoes.

2. The $\sqrt{1-\mathcal{A}}$ prefactor connects the ringdown reflectivity to the same absorptivity that governs inspiral heating, enforcing physical consistency between the two sectors.

3. The exponential factor provides frequency-dependent scrambling suppression:

[1] Strictly, $\mathcal{A} = 1$ adds the BH tidal heating contribution to a baseline that may or may not already include it. If the baseline waveform already incorporates horizon heating (as some recent models do [15]), $\mathcal{A}$ should be interpreted as a fractional deviation from the BH heating level rather than an absolute normalization. We retain the simpler interpretation here, as the toy inspiral baseline and most standard IMRPhenom models do not include BH-level heating by default.

high-frequency radiation interacting with the membrane is preferentially absorbed and scrambled, producing damped rather than persistent echoes.

4. The exponent δ reappears, linking the scrambling dynamics in the ringdown sector to the same microtexture that governs conservative tidal response.

We note that this reflectivity law produces weaker echoes than naive constant-reflectivity models, consistent with more realistic Teukolsky-based calculations that show weaker echo amplitudes than simple reflective-wall estimates [18].

D. Tapering rules

Smooth tapering windows confine each deformation to the sector where it is physically controlled:

a. Conservative tidal window.

$$W_\Lambda(f) = \frac{1}{2}\left[1 - \tanh\left(\frac{f - f_{\Lambda,\mathrm{off}}}{\sigma_\Lambda f_{\Lambda,\mathrm{off}}}\right)\right], \tag{14}$$

with $f_{\Lambda,\mathrm{off}} = 0.8\, f_{\mathrm{peak}}$ and $\sigma_\Lambda = 0.10$. This keeps the conservative finite-size correction predominantly in the inspiral regime.

b. Heating window. If the heating basis extends through merger (as in [15]), $W_{\mathcal{A}}(f) = 1$. Otherwise,

$$W_{\mathcal{A}}(f) = \frac{1}{2}\left[1 - \tanh\left(\frac{f - f_{\mathcal{A},\mathrm{off}}}{\sigma_{\mathcal{A}} f_{\mathcal{A},\mathrm{off}}}\right)\right], \tag{15}$$

with $f_{\mathcal{A},\mathrm{off}} = f_{\mathrm{peak}}$ and $\sigma_{\mathcal{A}} = 0.08$.

c. Ringdown transfer window.

$$W_R(f) = \frac{1}{2}\left[1 + \tanh\left(\frac{f - f_R}{\sigma_R f_R}\right)\right], \tag{16}$$

with $f_R = f_{220}$ (the dominant $\ell = m = 2$, $n = 0$ quasinormal mode frequency) and $\sigma_R = 0.12$.

These choices are model-design decisions, not literature values (see Fig. 2c for the window profiles). Their purpose is to ensure that the conservative correction is inspiral-dominated, the heating correction persists through merger if the basis supports it, and the cavity transfer function activates only near and beyond ringdown.

E. Summary: constitutive laws and their status

For clarity, we collect the three constitutive laws introduced in this work:

$$\Lambda_{\mathrm{eff}}(f) = \frac{\Lambda_\star}{|\ln\epsilon|}\,\frac{1}{1 + (2\pi f\,\tau_{\mathrm{c}})^\delta}, \tag{17}$$

$$R(f) = \sqrt{1 - \mathcal{A}}\,\exp\!\big[-(2\pi f\,\tau_{\mathrm{c}})^\delta\big], \tag{18}$$

$$\tau_{\mathrm{c}} = 4\,M_{\mathrm{f}}\,|\ln\epsilon|. \tag{19}$$

These are *toy-model closures*: phenomenologically motivated ansatze designed to connect effective membrane parameters to waveform observables in the simplest way consistent with known constraints. They are not derived from a specific microscopic theory of the membrane, and alternative functional forms are possible. The key physical content is the *structure* of the parameterization— four parameters mapping onto three observational channels—not the specific functional forms of Eqs. (17)–(19).

IV. PRIORS AND CONSISTENCY CONSTRAINTS

A. Recommended prior distributions

a. Compactness offset. We sample $x_\epsilon \equiv -\log_{10}\epsilon$ uniformly:

$$x_\epsilon \sim \mathrm{Uniform}(3, 20). \tag{20}$$

This covers membrane positions from $\epsilon = 10^{-3}$ (marginally compact) to $\epsilon = 10^{-20}$ (effectively Planckian for stellar-mass objects), while avoiding the numerically degenerate regime where only $|\ln\epsilon|$ matters.

b. Conservative response. A Cauchy shrinkage prior centered at zero:

$$p(\Lambda_\star) \propto \frac{1}{1 + (\Lambda_\star/\Lambda_0)^2}, \quad \Lambda_0 = 1, \tag{21}$$

optionally truncated at $|\Lambda_\star| < 20$. This encodes the expectation that BH-like objects should sit near zero conservative response while allowing departures of either sign.

c. Absorptivity. Either a flat discovery prior $\mathcal{A} \sim \mathrm{Uniform}(0, 1)$ or a conservative BH-leaning prior $\mathcal{A} \sim \mathrm{Beta}(4, 1.5)$, which gently favors high absorption.

d. Scrambling exponent.

$$\delta \sim \mathrm{Uniform}(0.25, 1.75). \tag{22}$$

B. Hard consistency cuts

Parameter draws are rejected if any of the following hold within the detector band:

1. $\max_f |\mathcal{T}(f)| > 1$: excludes overly resonant cavities.

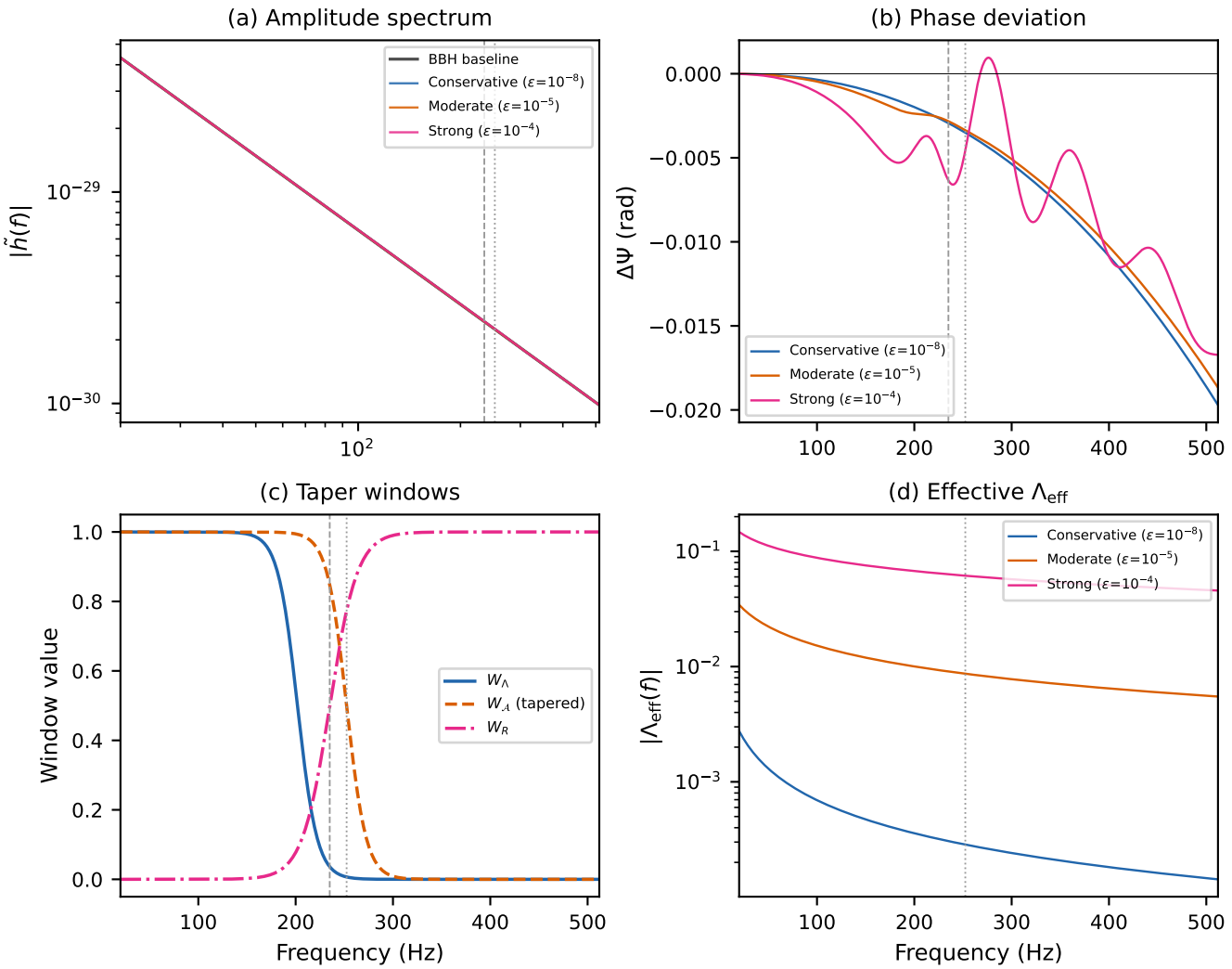

FIG. 2. NHSM waveform diagnostic for a GW150914-like system ($35 + 30\,M_\odot$, nonspinning). Three parameter sets are shown: conservative ($\epsilon = 10^{-8}$, $\Lambda_\star = 0.2$, $\mathcal{A} = 0.95$, $\delta = 1.0$; blue), moderate ($\epsilon = 10^{-5}$, $\Lambda_\star = 1.0$, $\mathcal{A} = 0.90$, $\delta = 0.7$; orange), and strong ($\epsilon = 10^{-4}$, $\Lambda_\star = 3.0$, $\mathcal{A} = 0.80$, $\delta = 0.5$; pink). **(a)** Amplitude spectrum; all three cases are nearly indistinguishable from the BBH baseline (black). **(b)** Phase deviation from the BBH baseline, dominated by the dissipative heating correction. **(c)** Taper windows confining each correction to its physical domain. Vertical lines mark $f_{\rm peak}$ (dotted) and f_{220} (dashed). **(d)** Frequency-dependent effective tidal deformability $\Lambda_{\rm eff}(f)$, showing the logarithmic compactness suppression and microtexture rolloff.

2. $\mathcal{A} < \mathcal{A}^{\rm min}(\chi_{\rm f})$: implements the spin-dependent ergoregion stability floor. We adopt the piecewise approximation $\mathcal{A}^{\rm min} \approx 0.003$ for $\chi_{\rm f} \leq 0.7$, ≈ 0.06 for $\chi_{\rm f} \leq 0.9$, and ≈ 0.60 for higher spins, following the ergoregion-instability analyses of [24].

3. $|\Lambda_{\rm eff}(f)| > \Lambda_{\rm max}$ over too much of the band: excludes nonperturbative conservative deformations.

4. $\tau_{\rm c}$ so large that all post-peak deviations move entirely outside the analyzed data window.

V. SYNTHETIC INJECTION AND MODEL BEHAVIOR

To demonstrate the model's behavior and verify its internal consistency, we generate synthetic NHSM waveforms for a GW150914-like system ($m_1 = 35\,M_\odot$, $m_2 = 30\,M_\odot$, nonspinning, $D_L = 410\,$Mpc) using a toy inspiral baseline with proper physical-unit scaling. The remnant parameters are $M_{\rm f} \approx 64.4\,M_\odot$, $\chi_{\rm f} \approx 0.65$, with characteristic frequencies $f_{\rm peak} \approx 252\,$Hz and $f_{220} \approx 235\,$Hz.

We compare three parameter sets spanning the model's dynamic range:

- **Conservative**: $\epsilon = 10^{-8}$, $\Lambda_\star = 0.2$, $\mathcal{A} = 0.95$, $\delta = 1.0$. This is the almost-BH corner.
- **Moderate**: $\epsilon = 10^{-5}$, $\Lambda_\star = 1.0$, $\mathcal{A} = 0.90$, $\delta = 0.7$.
- **Strong**: $\epsilon = 10^{-4}$, $\Lambda_\star = 3.0$, $\mathcal{A} = 0.80$, $\delta = 0.5$.

A. BH-recovery limit

Setting $\Lambda_\star = 0$ and $\mathcal{A} = 1$ (vanishing conservative response and perfect absorption), the NHSM waveform reduces to the BBH baseline to machine precision in amplitude: fractional differences are $\sim 10^{-16}$ across the entire frequency band. In phase, a residual shift of $\lesssim 0.02\,\mathrm{rad}$ remains. This is not a numerical artifact but a genuine physical effect: the heating correction $\Delta\Psi_{\mathcal{A}} = \mathcal{A}\,\Phi^{\rm lib}_{\rm heat}$ at $\mathcal{A} = 1$ adds the BH-level tidal heating contribution, which the toy inspiral baseline does not include by default. With a production baseline that already incorporates horizon heating (such as IMRPhenomD_Horizon [38]), the $\mathcal{A} = 1$ limit would produce exactly zero phase residual, or equivalently, $\mathcal{A}$ should be interpreted as a fractional deviation from the BH heating level in that context (see the footnote in Sec. III B 2).

B. Channel hierarchy

The diagnostic reveals a clear hierarchy among the three deformation channels (Figs. 2 and 3):

a. Dissipative heating. This is the dominant deviation channel in the conservative corner. Even at $\mathcal{A} = 0.95$ (near-BH absorption), the heating-induced phase shift accumulates to $\sim 0.002\,\mathrm{rad}$ through the inspiral. This is small but establishes the heating channel as the leading deformation sector; in the conservative corner, the Fisher analysis below (Sec. V D) indicates that this shift is not individually detectable for foreseeable single events, though it becomes the dominant target for population-level stacking. The shift grows with decreasing $\mathcal{A}$.

b. Conservative tidal response. The effective tidal deformability $\Lambda_{\rm eff}$ is suppressed by two factors: the logarithmic compactness prefactor $1/|\ln\epsilon| \approx 1/18$ for $\epsilon = 10^{-8}$, and the microtexture filter Ξ_δ which further suppresses the response at frequencies above $\sim 1/\tau_{\rm c} \approx 43\,\mathrm{Hz}$. As a result, the conservative phase correction is subdominant to the heating correction in the almost-BH regime.

c. Ringdown transfer function. For $\mathcal{A} \gtrsim 0.9$, the reflectivity $R(f)$ is small throughout the LIGO band. In the conservative case, $R \approx 0.01$ at 20 Hz and falls to $\lesssim 10^{-16}$ by the ringdown frequency. In the moderate case, $R \lesssim 10^{-4}$ at f_{220}. Consequently, the transfer function produces no appreciable amplitude or phase modification in these regimes. Only in the strong case ($\mathcal{A} = 0.80$, $\epsilon = 10^{-4}$) do cavity oscillations become visible, appearing as $\sim 0.5\%$ fractional amplitude modulations near the ringdown frequency.

This hierarchy is expected to be robust against changes in the baseline waveform. The suppression of the conservative tidal channel follows from the constitutive law itself: $\Lambda_{\rm eff}$ is reduced by $1/|\ln\epsilon|$ (a factor of $\sim 1/18$ for $\epsilon = 10^{-8}$) and further suppressed by the microtexture filter Ξ_δ above $f \sim 1/\tau_{\rm c}$. The suppression of the echo channel follows from the reflectivity law: $R(f)$ is exponentially damped by the scrambling factor for any $\mathcal{A} \gtrsim 0.9$. Neither suppression depends on the baseline amplitude or phase evolution. Verification with a calibrated baseline (IMRPhenomD or IMRPhenomXAS) is planned but the ordering is structurally expected within the present ansatz.

C. Observational implications

This channel hierarchy has a direct observational consequence: the NHSM model predicts that for objects in the almost-BH corner of parameter space, *the first observable deviation from BH behavior should appear in the dissipative heating channel, not in echoes or tidal deformability.* This is consistent with the current observational landscape, where echo searches have produced null results [21–23, 27], tidal deformability bounds are tight for binary neutron stars [19] and increasingly constraining for BBH events [37], but tidal heating constraints remain relatively loose [20, 38].

A full MCMC parameter-estimation study with realistic noise is deferred to future work. However, a phase-only Fisher-matrix estimate provides an order-of-magnitude assessment of detectability.

D. Fisher-matrix detectability forecast

We compute the 2×2 Fisher matrix for the two phase-dominant NHSM parameters $(\Lambda_\star, \mathcal{A})$ using the Newtonian inspiral amplitude and an analytic aLIGO design-sensitivity PSD for a GW150914-like source ($35 + 30\,M_\odot$, $D_L = 410\,\mathrm{Mpc}$), then rescale to specific target SNRs. The resulting 1σ measurement precisions are:

Configuration	$\sigma(\Lambda_\star)$	$\sigma(\mathcal{A})$	$\lvert\delta\mathcal{A}\rvert_{\rm cons}$
aLIGO (SNR 24)	~ 900	~ 13	0.004σ
O5 (SNR 100)	~ 210	~ 3	0.016σ
CE (SNR 300)	~ 70	~ 1	0.05σ
CE golden (SNR 1000)	~ 21	~ 0.3	0.16σ

Here $|\delta\mathcal{A}|_{\rm cons} = |1 - \mathcal{A}| = 0.05$ is the heating deviation in the conservative corner.

Three conclusions follow.

First, the ratio $\sigma(\Lambda_\star)/\sigma(\mathcal{A}) \approx 70$ is constant across the SNR range considered in this local forecast, providing a *quantitative* confirmation of the channel hierarchy: the heating channel constrains deviations from BH behavior

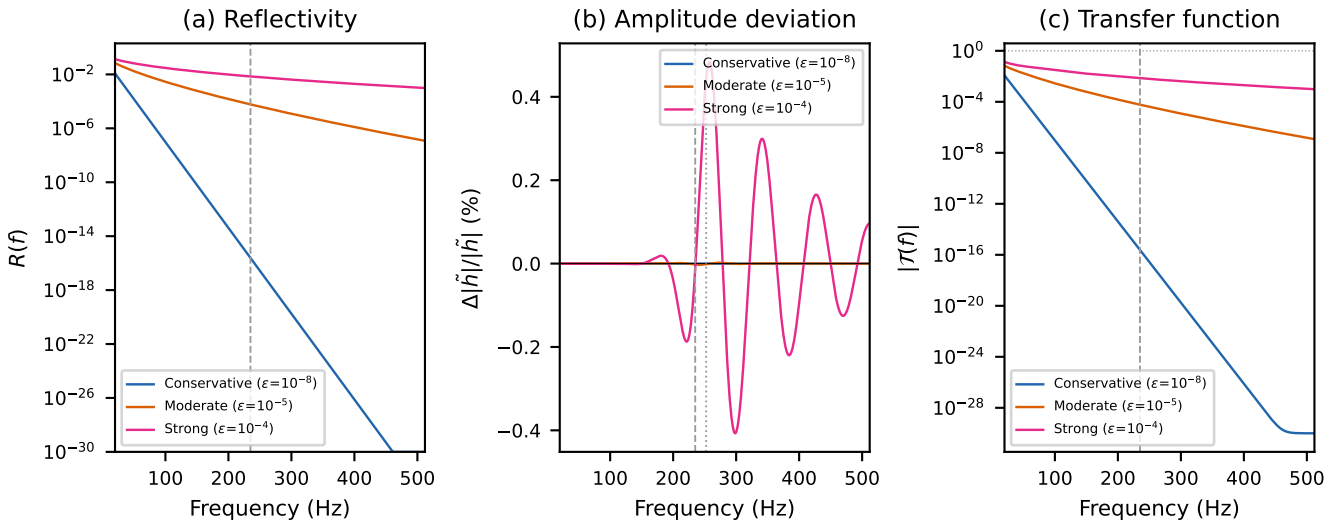

FIG. 3. Observational channel hierarchy for the three NHSM parameter sets of Fig. 2. **(a)** Membrane reflectivity $R(f)$: in the conservative corner ($\epsilon = 10^{-8}$, blue), the reflectivity is negligibly small across the entire LIGO band, falling to $\lesssim 10^{-16}$ at the ringdown frequency. **(b)** Fractional amplitude deviation from the BBH baseline: only the strong case ($\epsilon = 10^{-4}$, pink) shows sub-percent cavity oscillations near ringdown. **(c)** Transfer function amplitude: the conservative and moderate cases are many orders of magnitude below unity, confirming that the echo/transfer channel is inactive for almost-BH configurations.

roughly 70 times more tightly than the conservative tidal channel for this source class, across the SNR range considered.

Second, the conservative corner ($\Lambda_\star = 0.2$, $\mathcal{A} = 0.95$) is not individually detectable at any foreseeable single-event SNR. Even a CE golden event (SNR $\sim$ 1000) would measure the heating deviation at only $\sim 0.16\sigma$. This is consistent with the model's design: the almost-BH corner is meant to be hard to distinguish from a genuine BH. Population-level stacking across $O(10^3)$ or more CE-era events would be needed to reach the conservative corner.

Third, moderate deviations ($\mathcal{A} \lesssim 0.7$, $\Lambda_\star \gtrsim 10$) become accessible at CE sensitivities, and even current detectors can constrain the strong-deviation regime.

Caveats. This estimate uses a toy inspiral heating basis that grows as $\sim v^8$ and does not capture the steep phase accumulation near merger found by Mukherjee *et al.* [15, 38]. A production-quality Fisher matrix using their merger-capable approximant would likely reduce $\sigma(\mathcal{A})$ by a significant factor, potentially bringing the conservative corner within reach of CE-era population analyses. Similarly, marginalization over the full source-parameter space $(m_1, m_2, \chi_1, \chi_2, D_L, \iota)$ would increase the effective uncertainties; the values above are optimistic lower bounds. A complete Fisher or MCMC study with calibrated baselines is the highest-priority follow-up to this work.

VI. CONSTRAINTS FROM EXISTING DATA

The NHSM model is designed to live in a region of parameter space that is compatible with existing gravitational-wave observations. We now verify this explicitly against the three main constraint channels.

A. Tidal deformability bounds

The primary targets of the NHSM model are stellar-mass BBH systems. The phenomenological ECO-identifier framework of Ghosh and Hannam [37] finds that the compactness of GW150914 is consistent with black holes, and direct searches for nonzero tidal deformability in BBH events have yielded null results. For context, LVK analyses of the neutron-star binary GW170817 constrain the combined tidal deformability to $\tilde{\Lambda} \lesssim 800$ [19]; NHSM objects in the $\sim 30\,M_\odot$ range would have even smaller $\Lambda_{\rm eff}$ due to the mass scaling of the tidal phase basis.

For an NHSM object in the conservative corner ($\epsilon = 10^{-8}$, $\Lambda_\star = 0.2$), the effective tidal deformability at low frequencies is $\Lambda_{\rm eff} \approx \Lambda_\star/|\ln\epsilon| \approx 0.01$, which is far below current sensitivity. Even in the moderate case, $\Lambda_{\rm eff} \lesssim 0.1$, well within existing bounds. The NHSM model is thus trivially compatible with current tidal deformability constraints.

B. Tidal heating constraints

The recent analysis of Chia *et al.* [20] constrains the spin-independent tidal heating coefficient to $-13 < \mathcal{H}_0 < 20$ at 90% credibility using the LVK O1–O3 BBH catalog. At leading order, the NHSM absorptivity maps directly onto this coefficient: $\mathcal{A} \leftrightarrow \mathcal{H}_0$, with $\mathcal{A} = 1$ corresponding to $\mathcal{H}_0 = 1$ (the GR black hole value). The conservative corner of the NHSM model ($\mathcal{A} = 0.95$) therefore corresponds to $\mathcal{H}_0 \approx 0.95$, a deviation of 0.05 from unity — trivially within the current 90% credible interval. Even the strong case ($\mathcal{A} = 0.80$, $\mathcal{H}_0 \approx 0.8$) falls well within existing bounds. The Mukherjee *et al.* merger-capable heating approximant [15, 38] parameterizes the same physics through a horizon parameter H defined as the ratio of absorbed flux to the BH flux; $\mathcal{A}$ is a direct reparameterization of their H, with $\mathcal{A} = 1$ mapping to $H = H_{\rm BH}$ and $\mathcal{A} = 0$ to the no-horizon limit. The NHSM model adds to their framework by connecting $\mathcal{A}$ to the ringdown reflectivity through the same parameter, enforcing consistency between the inspiral and postmerger sectors.

The current bounds are prior-dominated for most events, with $|\mathcal{H}_0| \lesssim 100$ excluded for the best events. The merger-capable approximant of Mukherjee *et al.* [15] will further tighten these constraints by extending the heating model through the strong-gravity regime.

C. Echo search null results

Multiple searches for gravitational-wave echoes in the LVK data have produced null results [21–23, 27]. The NHSM model is compatible with these null results by construction: in the almost-BH corner, the reflectivity $R(f)$ is exponentially suppressed by the scrambling factor $\exp[-(2\pi f\,\tau_{\rm c})^{\delta}]$, producing echoes that are many orders of magnitude below current detection thresholds.

More precisely, for $\epsilon = 10^{-8}$ and $\mathcal{A} = 0.95$ ($\sqrt{1-\mathcal{A}} \approx 0.22$), the reflectivity at 20 Hz is $R \approx 0.01$, and it falls to $R \sim 10^{-16}$ by the ringdown frequency. Despite the non-negligible low-frequency reflectivity, the transfer function is inactive there because the ringdown window $W_R(f)$ suppresses contributions below f_{220}. At the frequencies where the transfer function operates, echoes are effectively unmeasurable. This is a feature of the model's dissipative design: a scrambling membrane naturally produces weak echoes because it absorbs and thermalizes rather than coherently reflecting.

D. Prospects for next-generation detectors

The primary discrimination channel for NHSM objects will be tidal heating. The Cosmic Explorer and Einstein Telescope facilities, with an order of magnitude improvement in low-frequency sensitivity, could tighten heating constraints by up to roughly two orders of magnitude. At that level, NHSM deviations with $\mathcal{A} \lesssim 0.99$ may become measurable for high-SNR BBH events. The conservative tidal response channel becomes competitive only for objects with $\epsilon \gtrsim 10^{-5}$ (moderate compactness), and the echo channel requires $\mathcal{A} \lesssim 0.8$ to produce detectable late-time structure.

VII. DISCUSSION

A. Relationship to existing literature

The NHSM model draws on and extends several strands of the ECO literature:

The *membrane paradigm* [28] provides the conceptual foundation: an effective dissipative surface at (or near) the horizon that absorbs and thermalizes infalling flux. The recent extension to tidal deformability by Silvestrini *et al.* [16] develops a model-agnostic framework in which the tidal properties of any spherically symmetric compact object are encoded through frequency-dependent bulk and shear viscosity coefficients of a fictitious membrane. The NHSM constitutive law for $\Lambda_{\rm eff}(f)$ [Eq. (17)] corresponds to a specific, minimal choice within this framework: the microtexture filter Ξ_δ plays the role of a frequency-dependent viscosity profile, and the $1/|\ln\epsilon|$ compactness suppression is consistent with the logarithmic scaling they identify for ultracompact objects approaching the BH limit. The NHSM model adds to their framework by providing an explicit waveform-facing parameterization that connects the tidal sector to the dissipative (heating) and ringdown (transfer function) sectors through a shared set of effective parameters—something the Silvestrini *et al.* formalism does not address, as it focuses on the conservative tidal response alone.

The *gravastar* literature [3, 4] provides the spacetime architecture: exterior Schwarzschild/Kerr, interior de Sitter-like vacuum, with a transition layer. The NHSM membrane corresponds to this transition layer, but with two key differences: it is dissipative rather than rigid, and its microstructure is parameterized by the scrambling exponent δ rather than by a specific equation of state.

The *echo/transfer-function* formalism [8, 17, 18] provides the ringdown sector. The NHSM transfer function is a specific case of the general ECO cavity transfer function, with the frequency-dependent reflectivity (13) replacing the constant or slowly varying reflectivity used in many echo searches.

The *tidal heating* literature [13–15, 20, 38] provides the dissipative inspiral sector. The NHSM heating correction uses the same phase basis as existing heating-enabled waveform models, scaled by the absorptivity $\mathcal{A}$.

The *ECO-identifier* approach of Ghosh and Hannam [37] shares the NHSM model's philosophy of phenomenological compactness parameterization, but operates with a single additional parameter

(compactness) rather than four. The NHSM model provides finer-grained discrimination: two objects with the same compactness ϵ but different absorptivities $\mathcal{A}$ would be indistinguishable in the Ghosh-Hannam framework but produce different heating signatures in the NHSM model. More broadly, the single-compactness approach captures the *where* of a near-horizon surface (how close it sits to the would-be horizon) but not the *how* (whether it absorbs, reflects, or scrambles). The NHSM parameterization encodes both.

B. What the model does and does not claim

The NHSM model claims to be:

- A compact, testable, phenomenologically motivated deformation of standard BBH waveform templates.
- Designed to encode "no entry + absorption + scrambling" physics in a form compatible with existing waveform infrastructure.
- A model in which the conservative limit ($\mathcal{A} \approx 1$, $\Lambda_\star \approx 0$) cleanly recovers BH behavior.
- A parameterization whose four parameters map onto three distinct observational channels.

The model does *not* claim:

- That astrophysical black holes are actually NHSM objects.
- That the constitutive laws are derived from first principles, or that they are unique. Alternative functional forms consistent with the same physical constraints may produce quantitatively different but qualitatively similar observational signatures. The key content of the model is the parameterization structure—four parameters, three channels—not the specific closures.
- That echoes have been detected or are likely to be detected.
- That the model replaces GR or provides a complete theory of the horizon.

C. The "no entry" versus "no return" distinction

The classical event horizon is a *point of no return*: once crossed, nothing—not matter, not light, not information—can escape. The NHSM membrane is a *point of no entry*: infalling flux is intercepted at $r_{\rm m}$, absorbed by the membrane's effective degrees of freedom, and scrambled on a timescale $t_{\rm scr} \sim \beta \ln S$.

This distinction matters observationally because a "no entry" boundary can, in principle, affect the inspiral dynamics through finite-size effects (tidal deformability and heating) and modify the ringdown through partial reflection. A "no return" boundary, by definition, can produce neither. The NHSM parameterization provides a minimal framework for quantifying the observational consequences of this distinction.

D. Parameter correlations and minimality

The absorptivity parameter $\mathcal{A}$ appears in both the inspiral heating correction and the ringdown reflectivity. This creates a physical correlation between the two sectors: an object that absorbs less during inspiral (lower $\mathcal{A}$) will also reflect more during ringdown (higher R). This correlation is a feature, not a bug—it enforces physical consistency and reduces the effective dimensionality of the parameter space for inference.

Similarly, the compactness offset ϵ controls the cavity timescale $\tau_{\rm c}$, which in turn determines both the compactness-suppression of the tidal response and the echo delay time. This means that a single parameter governs the "compactness" of the object across all three sectors. The four-parameter set $\{\epsilon, \Lambda_\star, \mathcal{A}, \delta\}$ is therefore close to the minimum needed to independently probe conservative response, dissipative response, and microstructure dynamics.

A further structural choice in the minimal model is that the scrambling exponent δ appears in both the conservative tidal filter Ξ_δ [Eq. (10)] and the ringdown reflectivity [Eq. (13)]. This single-exponent assumption is a leading-order closure: one microstructure parameter governs both sectors. The natural extension is a two-exponent model $(\delta_\Lambda, \delta_R)$ with a prior favoring near-equality, so that data can determine whether a single microstructure exponent genuinely controls both the conservative and dissipative response channels, or whether the two sectors require independent spectral parameters. We retain the single-δ form here as the minimal testable model.

E. Open questions

Several important questions remain beyond the scope of this phenomenological model:

Dynamical stability. The NHSM model specifies the membrane's effective parameters but does not demonstrate that a self-consistent solution of the Einstein equations with the prescribed membrane stress-energy is dynamically stable. Radial and nonradial stability analyses, analogous to those performed for thin-shell gravastars [4], would be needed to establish viability.

Formation channels. The model is agnostic about how an NHSM object would form astrophysically. Candidate formation channels include quantum-gravitational modifications to the endpoint of gravitational collapse, or phase transitions in the near-horizon regime.

Full numerical relativity. The NHSM waveform is a perturbative deformation of a BBH baseline. A fully self-consistent treatment would require numerical relativity simulations of merging NHSM objects, which is beyond current computational capabilities for generic ECOs.

Spinning objects. The current model treats aligned-spin systems with the ergoregion stability constraint as a prior cut. A more complete treatment would include spin-dependent modifications to the constitutive laws and taper parameters. The recent extension of the membrane paradigm to slowly spinning horizonless compact objects [26] provides the formal framework for such an extension, including spin-dependent reflectivity and QNM structure that could inform spin-modified constitutive laws.

Operator-informed constitutive laws. The three constitutive laws proposed here are minimal phenomenological closures. A more principled approach would derive the functional forms from the spectral properties of a boundary operator on the membrane surface—for instance, linking the scrambling exponent δ to a spectral dimension or anomalous diffusion exponent of the membrane's graph Laplacian, and linking the absorptivity $\mathcal{A}$ to an attenuation functional of the boundary's heat-kernel trace. Such an operator-level reformulation would replace the current ad hoc closures with mathematically controlled families, and would also provide a principled basis for determining whether the single-δ assumption holds or whether the conservative and reflectivity sectors require independent spectral exponents.

VIII. CONCLUSION

We have presented the Near-Horizon Scrambling Membrane (NHSM) model: a four-parameter phenomenological waveform deformation designed to test whether the compact objects observed in gravitational-wave mergers possess dissipative, absorptive boundary layers in place of classical event horizons.

The model's key features are:

(i) It parameterizes the almost-BH corner of the ECO parameter space through four physically motivated quantities: compactness offset ϵ, conservative response $\Lambda_\star$, absorptivity $\mathcal{A}$, and scrambling exponent δ.

(ii) These parameters map cleanly onto three distinct observational channels—conservative inspiral dephasing, dissipative heating, and ringdown transfer structure—allowing the three physical sectors to be probed and constrained separately.

(iii) Three constitutive laws [Eqs. (17)–(19)] connect effective membrane parameters to waveform observables in the simplest way consistent with known constraints from ergoregion stability, Love-number suppression, and fast scrambling.

(iv) In the conservative corner, the primary deviation channel is dissipative heating rather than tidal deformability or echoes, consistent with the current observational landscape. A Fisher-matrix forecast quantifies this: the heating channel constrains deviations $\sim$ 70 times more tightly than the conservative tidal channel for stellar-mass BBH sources.

(v) The model is fully compatible with existing LVK constraints from tidal deformability analyses, tidal heating bounds, and echo search null results.

The distinctive observational claim of the NHSM model is not the generic existence of echoes, but a correlated hierarchy of small deviations in which dissipative inspiral-merger effects emerge before conservative finite-size effects, and both precede any appreciable late-time recycled signal.

The NHSM parameterization provides a compact, falsifiable framework for probing the "no entry versus no return" distinction at the horizon scale. With the merger-capable heating models now available [15, 38] and the sensitivity improvements expected from O5 and next-generation detectors, the dissipative channel identified here as the primary NHSM observable will become increasingly constraining.

The model's constitutive laws are intentionally phenomenological. As theoretical understanding of near-horizon microphysics advances and observational constraints tighten, these toy closures can be replaced with more physically grounded relations while preserving the four-parameter structure. The value of the NHSM framework lies not in the specific functional forms, but in the organizational principle: four parameters, three channels, one operational question—is the would-be horizon observationally indistinguishable from a one-way causal surface, or does it behave as a dissipative near-horizon boundary layer?

ACKNOWLEDGMENTS

The author thanks colleagues and AI-assisted research collaborators for support in model formalization, code prototyping, literature organization, figure refinement, and editorial review. All scientific judgments, claim selection, interpretation, and responsibility for the final manuscript remain with the author.

Appendix A: Implementation Details

A reusable Python implementation of the NHSM waveform model is available as the `nhsm_waveform` package. The code is structured around an abstract baseline interface (`BaselineWaveform`) that can be backed by any frequency-domain BBH waveform generator. Three backends are provided:

- `ToyInspiralBaseline`: a lightweight Newtonian-like inspiral waveform with crude

remnant fits, suitable for testing the NHSM deformation logic in isolation. This backend uses geometric units internally and requires MTSUN conversion for physical-frequency applications.

- `PyCBCBaseline`: an adapter wrapping `pycbc.waveform.get_fd_waveform()`, supporting any PyCBC-available approximant (e.g., IMRPhenomD, IMRPhenomXAS). Masses in solar masses, distance in Mpc.
- `LALSimulationBaseline`: an adapter wrapping `SimInspiralChooseFDWaveform()`, with automatic unit conversion to SI.

An `AutoBaseline` factory selects the best available backend at runtime. The tidal and heating phase bases currently use proxy PN-like functions; replacing these with calibrated library-backed bases is the primary recommended upgrade for production use.

The four NHSM parameters are encapsulated in a `NHSMParams` dataclass. The `NHSMWaveform` class provides:

- `h_tilde(f, src, nhsm)`: the full NHSM waveform, Eq. (7).
- `valid(f, src, nhsm)`: a Boolean consistency check implementing the hard cuts of Sec. IV B.
- `log_prior(nhsm)`: an example shrinkage prior implementing the distributions of Sec. IV A.

The synthetic injections in Sec. V were produced using the toy baseline with MTSUN-corrected frequency scaling. The corrected diagnostic script and all figure-generation code are included with the package. The `nhsm_waveform` code will be made publicly available upon publication.

[1] B. P. Abbott *et al.* (LIGO Scientific Collaboration and Virgo Collaboration), Observation of Gravitational Waves from a Binary Black Hole Merger, Phys. Rev. Lett. **116**, 061102 (2016).
[2] S. W. Hawking, Breakdown of predictability in gravitational collapse, Phys. Rev. D **14**, 2460 (1976).
[3] P. O. Mazur and E. Mottola, Gravitational vacuum condensate stars, Proc. Nat. Acad. Sci. **101**, 9545 (2004).
[4] C. Cattoen, T. Faber, and M. Visser, Gravastars must have anisotropic pressures, Class. Quantum Grav. **22**, 4189 (2005).
[5] I. Bena and D. R. Mayerson, Black holes, black rings, and their microstates, Lect. Notes Phys. **1005**, 1 (2022).
[6] A. Almheiri, D. Marolf, J. Polchinski, and J. Sully, Black holes: Complementarity vs. firewalls, J. High Energy Phys. **02**, 062 (2013).
[7] L. Susskind, L. Thorlacius, and J. Uglum, The stretched horizon and black hole complementarity, Phys. Rev. D **48**, 3743 (1993).
[8] V. Cardoso, E. Franzoni, and P. Pani, Is the gravitational-wave ringdown a probe of the event horizon?, Phys. Rev. Lett. **116**, 171101 (2016).
[9] V. Cardoso and P. Pani, Tests for the existence of black holes through gravitational wave echoes, Nat. Astron. **1**, 586 (2017).
[10] T. Damour and S. N. Solodukhin, Wormholes as black hole foils, Phys. Rev. D **76**, 024016 (2007).
[11] T. Binnington and E. Poisson, Relativistic theory of tidal Love numbers, Phys. Rev. D **80**, 084018 (2009).
[12] A. Le Tiec, M. Casals, and E. Franzini, Tidal Love Numbers of Kerr Black Holes, Phys. Rev. D **103**, 084021 (2021).
[13] S. Datta, R. Brito, S. Bose, P. Pani, and S. A. Hughes, Tidal heating as a discriminator for horizons in extreme mass ratio inspirals, Phys. Rev. D **101**, 044004 (2020).
[14] H. S. Chia, Tidal deformation and dissipation of rotating black holes, Phys. Rev. D **109**, 024030 (2024).
[15] S. Mukherjee, S. Datta, S. Bose, and K. S. Phukon, Binary black holes in the heat of merger, arXiv:2506.22363 [gr-qc] (2025).
[16] M. Silvestrini, E. Maggio, S. Chakraborty, and P. Pani, One membrane to Love them all: Tidal deformations of compact objects from the membrane paradigm, Phys. Rev. D **112**, 124021 (2025); arXiv:2506.16516.
[17] Z. Mark, A. Zimmerman, S. M. Du, and Y. Chen, A recipe for echoes from exotic compact objects, Phys. Rev. D **96**, 084002 (2017).
[18] E. Maggio, A. Testa, V. Cardoso, and P. Pani, Analytical model for gravitational-wave echoes from spinning remnants, Phys. Rev. D **100**, 064056 (2019).
[19] B. P. Abbott *et al.* (LIGO Scientific Collaboration and Virgo Collaboration), GW170817: Measurements of Neutron Star Radii and Equation of State, Phys. Rev. Lett. **121**, 161101 (2018).
[20] H. S. Chia, Z. Zhou, and M. M. Ivanov, Bring the heat: Tidal heating constraints for black holes and exotic compact objects from the LIGO-Virgo-KAGRA data, arXiv:2404.14641 [gr-qc] (2024).
[21] J. Abedi, H. Dykaar, and N. Afshordi, Echoes from the abyss: Tentative evidence for Planck-scale structure at black hole horizons, Phys. Rev. D **96**, 082004 (2017).
[22] J. Westerweck *et al.*, Low significance of evidence for black hole echoes in gravitational wave data, Phys. Rev. D **97**, 124037 (2018).
[23] R. Abbott *et al.* (LIGO Scientific Collaboration, Virgo Collaboration, and KAGRA Collaboration), Search for gravitational-wave signals associated with ultracompact objects, Phys. Rev. D **104**, 082002 (2021).
[24] E. Maggio, V. Cardoso, S. R. Dolan, and P. Pani, Ergoregion instability of exotic compact objects: ultracompact stars and quantum corrections at the horizon scale, Phys. Rev. D **99**, 064007 (2019).
[25] E. Maggio, P. Pani, and V. Ferrari, Exotic compact objects and how to quench their ergoregion instability, Phys. Rev. D **96**, 104047 (2017).
[26] M. V. S. Saketh and E. Maggio, Quasinormal modes of

slowly-spinning horizonless compact objects, Phys. Rev. D **110**, 084030 (2024); arXiv:2406.10070.
[27] K. W. Tsang, A. Ghosh, A. Samajdar, K. Chatziioannou, S. Mastrogiovanni, M. Agathos, and C. Van Den Broeck, A morphology-independent search for gravitational wave echoes in data from the first and second observing runs of Advanced LIGO and Advanced Virgo, Phys. Rev. D **101**, 064012 (2020).
[28] K. S. Thorne, R. H. Price, and D. A. Macdonald, *Black Holes: The Membrane Paradigm* (Yale University Press, New Haven, 1986).
[29] W. Israel, Singular hypersurfaces and thin shells in general relativity, Nuovo Cim. B **44**, 1 (1966); Erratum: **48**, 463 (1967).
[30] Y. Sekino and L. Susskind, Fast scramblers, J. High Energy Phys. **10**, 065 (2008).
[31] J. Maldacena, S. H. Shenker, and D. Stanford, A bound on chaos, J. High Energy Phys. **08**, 106 (2016).
[32] P. Hayden and J. Preskill, Black holes as mirrors: Quantum information in random subsystems, J. High Energy Phys. **09**, 120 (2007).
[33] J. D. Bekenstein, Black holes and entropy, Phys. Rev. D **7**, 2333 (1973).
[34] S. W. Hawking, Particle creation by black holes, Commun. Math. Phys. **43**, 199 (1975).
[35] V. Cardoso, E. Franzoni, A. Maselli, P. Pani, and G. Raposo, Testing strong-field gravity with tidal Love numbers, Phys. Rev. D **95**, 084014 (2017); Erratum: **95**, 089901 (2017).
[36] P. Pani, I-Love-Q relations for gravastars and the approach to the black-hole limit, Phys. Rev. D **92**, 124030 (2015).
[37] S. Ghosh and M. Hannam, On the identification of exotic compact binaries with gravitational waves: a phenomenological approach, Phys. Rev. D **112**, 104017 (2025); arXiv:2505.16380.
[38] S. Mukherjee, S. Datta, S. Bose, and S. K. Phukon, IMRPhenomD_Horizon: A frequency-domain gravitational waveform model incorporating horizon fluxes, Phys. Rev. D **110**, 124027 (2024).
[39] R. Metzler and J. Klafter, The random walk's guide to anomalous diffusion: a fractional dynamics approach, Phys. Rep. **339**, 1 (2000).